SLOW COMPRESSIONAL WAVE IN POROUS MEDIA: FINITE DIFFERENCE SIMULATIONS ON MICRO-SCALE

E.H. Saenger, R. Ciz, B. Gurevich, and S.A. Shapiro

email: *saenger@geophysik.fu-berlin.de*
keywords: *poroelasticity, Biot's theory, slow wave, finite-differences*

ABSTRACT

We perform wave propagation simulations in porous media on microscale in which a slow compressional wave can be observed. Since the theory of dynamic poroelasticity was developed by Biot (1956), the existence of the type II or Biot's slow compressional wave (SCW) remains the most controversial of its predictions. However, this prediction was confirmed experimentally in ultrasonic experiments. The purpose of this paper is to observe the SCW by applying a recently developed viscoelastic displacement-stress rotated staggered finite-difference (FD) grid technique to solve the elastodynamic wave equation. To our knowledge this is the first time that the slow compressional wave is simulated on first principles.

INTRODUCTION

One of the key predictions of Biot's theory of poroelasticity (Biot, 1956) is the fact that in a poroelastic medium, there may propagate elastic waves of three types: a shear wave and two types of compressional waves. The first compressional wave is the one that is very similar to the compressional wave in an elastic medium, while the second wave, also called type II or Biot's slow wave, has a strongly dispersive character. At low frequencies, at which the flow of the pore fluid is characterized by the Poiseuille flow, the slow wave has a diffusion-type character. At higher frequencies, when the viscous skin depth of the fluid in the pores is smaller than the size of the pores, the slow wave becomes a normal propagating wave with small attenuation, and can be approximately described as an acoustic wave in the pore fluid.
The slow wave at higher frequencies was confirmed experimentally, when the SCW was observed in ultrasonic experiments by Plona (1980). Theoretical analysis, e.g. by Dutta (1980), shows that the observed travel times of the SCW are consistent with the predictions of Biot's theory.
Goal of this study is to observe numerically the SCW on first principles (i.e. by solving the elastodynamic wave equation) and not by solving Biot's equations of poroelasticity [e.g.; Dai et al. (1995); Gurevich et al. (1999)]. This is done in 2D with a comparison to an analytical solution as well as in 3D numerical experiments. We apply a recently developed viscoelastic displacement-stress rotated staggered finite-difference (FD) grid technique (Saenger et al., 2005).

2D NUMERICAL EXPERIMENTS

We consider a system of periodically alternating solid and fluid layers of period d (Figure 1). The elastic solid has density ρ_s, bulk modulus K_s and shear modulus μ_s. The viscous fluid has densityρ_f, bulk modulus (inverse compressibility) K_f, and dynamic viscosity η. The solid and fluid layer thicknesses are h_s and h_f, respectively, so that $h_s + h_f = d$.
Propagation of compressional waves in a periodic system of solid layers denoted by s and f is governed

by an exact dispersion equation (Rytov, 1956; Brekhovskikh, 1981; Gurevich, 2002):

$$\begin{aligned} &4(\mu_s-\mu_f)^2K_1K_2+\omega^2\rho_s\left[c^2\rho_s-4\left(\mu_s-\mu_f\right)\right]K_2\tan\tfrac{\beta_s h_s}{2}\\ &+\omega^2\rho_f\left[c^2\rho_f+4\left(\mu_s-\mu_f\right)\right]K_1\tan\tfrac{\beta_f h_f}{2}\\ &-\omega^2\rho_f\rho_s c^2\left[L_1\tan\tfrac{\beta_f h_f}{2}+L_2\tan\tfrac{\beta_s h_s}{2}\right]=0, \end{aligned} \tag{1}$$

where $\alpha_s^2=\omega^2\left(1/c_s-1/c\right)$, $\alpha_f^2=\omega^2\left(1/c_f-1/c\right)$ and $c_s=\left[(K_s+4\mu_s/3)/\rho_s\right]^{1/2}$, $c_f=\left[(K_f+4\mu_f/3)/\rho_f\right]^{1/2}$ are compressional velocities in the materials s and f, respectively, $Im\mu_f=Im\lambda_f=-\omega\eta$, $K_f=\lambda_f+2\mu_f/3$ and

$$\begin{aligned} K_1&=\tfrac{\omega^2}{c^2}\tan\tfrac{\beta_s h_s}{2}+\alpha_s\beta_s\tan\tfrac{\alpha_s h_s}{2},\\ K_2&=\tfrac{\omega^2}{c^2}\tan\tfrac{\beta_f h_f}{2}+\alpha_f\beta_f\tan\tfrac{\alpha_f h_f}{2},\\ L_1&=\tfrac{\omega^2}{c^2}\tan\tfrac{\beta_s h_s}{2}-\alpha_f\beta_s\tan\tfrac{\alpha_f h_f}{2},\\ L_2&=\tfrac{\omega^2}{c^2}\tan\tfrac{\beta_f h_f}{2}-\alpha_s\beta_f\tan\tfrac{\alpha_s h_s}{2}. \end{aligned} \tag{2}$$

Equation (1) needs to be analysed on the macroscale, that is in the limit $|\omega d/c|\ll 1$. However such a theoretical analysis appears to be too involved, and the analytical solution is only known in the low-frequency limit (Gurevich, 2002). It has been shown numerically (Bedford, 1986), that for sufficiently small values of $|\omega d/c|$ attenuation and dispersion predicted by equation (1) are the same as given by Biot's dispersion equation. Note that both equation (1) and Biot's theory predict both types of compressional waves (the fast compressional wave and Biot's slow wave).

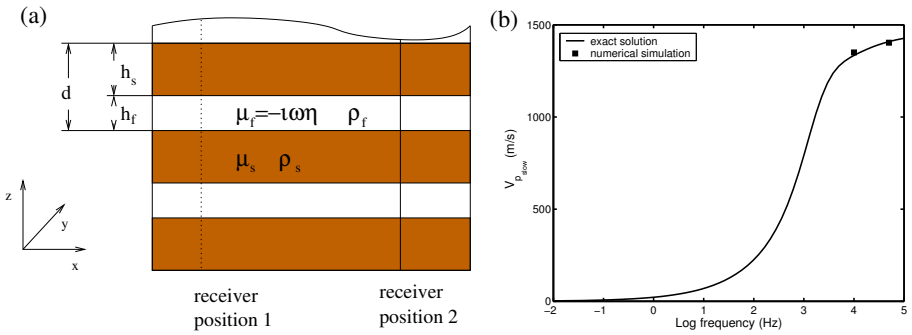

Figure 1: Left hand side (a): Medium of alternating solid and viscous fluid layers. **Right** hand side (b): Numerical (dots) vs. analytical solution (solid line) for the velocity of the SCW in the medium shown on the left hand side. An excellent agreement is observed.

To obtain the effective velocities of slow waves in layered media we choose the following numerical setup. The synthetic model contains two horizontal thin layers of viscous fluid and elastic solid of equal size (30x3000 grid points with an interval of Δx=0.0001 m). The solid has the P-wave velocity v_p=5100 m/s, S-wave velocity v_s=2944 m/s, density ρ_s=2540 kg/m^3 and viscosity η=0 kg/m.s. For the viscous fluid we set c_{11}=3.922*10^{11}, c_{44}=1.3*10^{11} , and ρ_f=1000 kg/m^3. The fluid viscosity $\eta=10\ kg/(ms)$ is determined with the choice of $\omega_1=1.3*10^{10}$ [see Saenger et al. (2005) for details]. To generate a slow-wave in x-direction (f_{dom}=50 kHz or f_{dom}=10 kHz), we apply a line source in z-direction in the fluid and perform the finite-difference simulations with periodic boundary conditions (in z-direction). The effective velocity is estimated by measuring the time of the zero-crossing of the plane wave over a distance of 1000 grid points (distance between receiver position 1 and 2; see Figure 1). All computations are carried out with the second order spatial FD operators and with the second order time update. The results are shown in Figure 1.

3D NUMERICAL EXPERIMENTS

To observe a slow wave in a realistic 3D porous solid we perform simulations with a numerical setup similar to the experiments described in Saenger et al. (2005). We apply the 3D RSG-technique to explicitely

model wave propagation in fluid saturated porous media. The synthetic porous rock-models are embedded in a homogeneous fluid region. The full models are made up of 600x400x400 grid points with an interval of Δx=0.0002m. For the grain material we set a P-wave velocity of v_p=5100m/s, a S-wave velocity of v_s=2944m/s and a density of ρ_{grain}=2540kg/m^3. For the fluid we set v_p=1500m/s, v_s=0m/s and ρ_v=1000kg/m^3. We perform our modeling experiments with periodic boundary conditions in the two horizontal directions. We apply a plane source at the top of the model. The plane P-wave generated in this way propagates from the top of the model to the interface of fluid and fluid-saturated porous media. The source wavelet is the first derivative of a Gaussian with a dominant frequency of $f_{source} = 8 \times 10^4 Hz$ and with a time increment of $\Delta t = 2.1 * 10^{-8} s$. All computations are performed with second order spatial FD operators and with a second order time update.

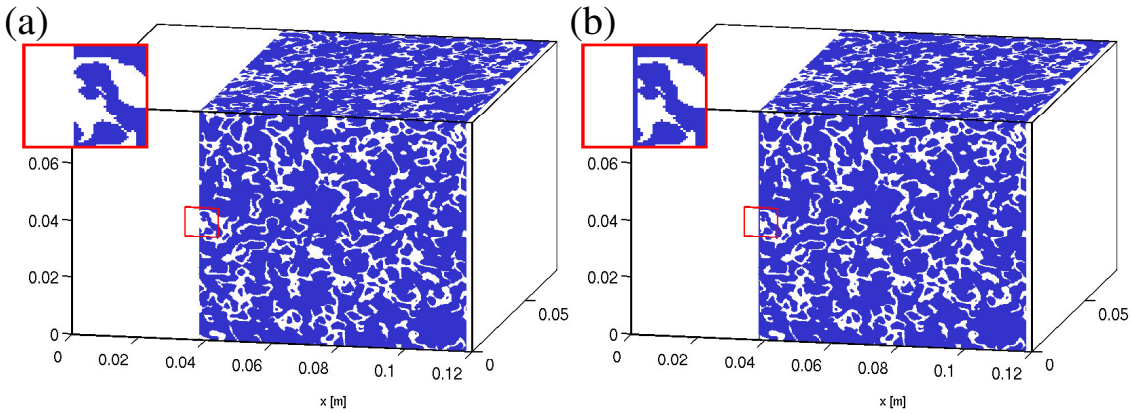

Figure 2: Two different 3D synthetic porous models. The pore structure is defined by the synthetic rock model GRF5 (see Saenger et al. (2005) for details). White regions indicates water; blue regions indicates grain material. **Left** hand side (a): Open pores at the interface (x-position $\approx$ 0.4m). **Right** hand side (b): Sealed conditions (a very thin solid layer) at the same interface.

For the model shown in Figure 2a the incident P-wave generates from a theoretical point of view (Gurevich et al., 2004) one reflected and two transmitted compressional waves (fast and slow). The reflected P-wave and the transmitted fast P-wave can be detected very clearly from a 2D slice from a snapshot of the full 3D wavefield (Figure 3a). The transmitted slow P-wave can only be seen by calculating the average displacement field as shown in Figure 4a.

An analysis based on the boundary conditions at an interface for Biot's equations of poroelasticity shows that the slow wave is generated if and only if there exist at least a hydraulic contact between the free water and the water in the pore space [e.g. (Rasolofosaon, 1980)]. Therefore we repeat the previously described simulation with a small modification: We create a very thin solid layer at the interface between fluid and fluid-saturated porous media (Figure 2b). As expected a slow wave can not be observed in such a simulation as shown in Figure 4b.

CONCLUSIONS

We have performed numerical modeling of seismic wave propagation on a micro-scale. A compressional slow wave (a Biot type II wave) is observed in 2D and 3D simulations. In both cases we compare our results with theoretical predictions successfully. This confirms that the viscoelastic rotated staggered grid FD method of Saenger et al. (2005) is capable of modelling poroelastic (associated with global flow) effects with high accuracy. To our knowledge this is the first time that the slow wave is simulated on first principles.

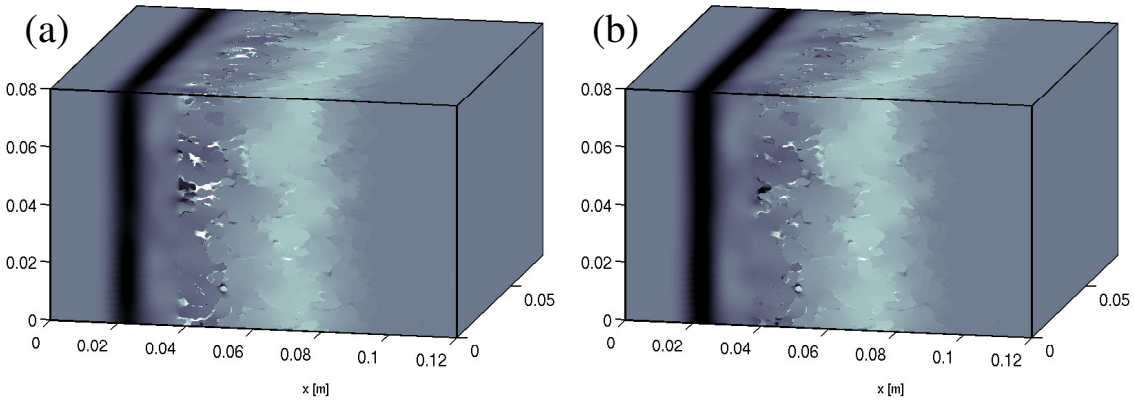

Figure 3: A z-displacement snapshot of the wavefield after 2100 timesteps. The reflected P-wave (at x ≈ 0.02m) and the transmitted fast P-wave (at x ≈ 0.07m) are clearly visible. **Left** hand side (a): Snapshot for the model with open pores at the interface (Figure 2a). **Right** hand side (b): Same as (a) but with for the model with a sealed interface (Figure 2b).

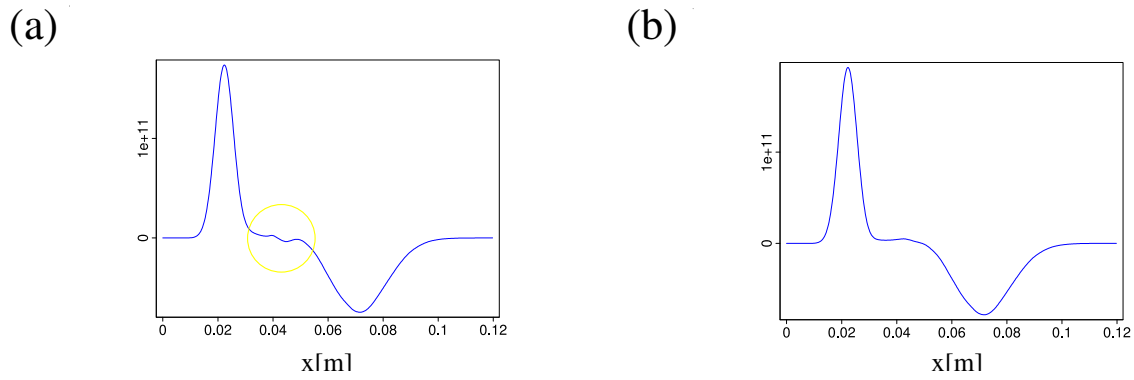

Figure 4: Average of the z-displacement-field after 2100 timesteps and after the incident P-wave was partly reflected and transmitted at the interface at x= ≈ 0.04m. **Left** hand side (a): A slow compressional wave can be observed (marked with a circle) using the model shown in Figure 2a). **Right** hand side (b): The slow wave is not generated using the model shown in Figure 2b.

REFERENCES

Bedford, A. (1986). Application of Biot's equations to a medium of alternating fluid and solid layers. *J. Wave-Material Interaction*, 1:34–53.

Biot, M. A. (1956). Theory of propagation of elastic waves in a fluid-saturated porous solid. I. Low frequency range and II. Higher-frequency range. *J. Acoust. Soc. Amer.*, 28:168–191.

Brekhovskikh, L. M. (1981). *Waves in layered media*. Academic Press.

Dai, N., Vafidis, A., and Kanasewich, E. R. (1995). Wave propagation in heterogeneous, porous media: A velocity-stress, finite-difference method. *Geophysics*, 60:327–340.

Dutta, N. C. (1980). Theoretical analysis of observed second bulk compressional wave in a fluid-saturated porous solid at ultrasonic frequencies. *Appl. Phys. Lett.*, 37:898–900.

Gurevich, B. (2002). Effect of fluid viscosity on elastic wave attenuation in porous rocks. *Geophysics*, 67:264–270.

Gurevich, B., Ciz, R., and Dennemann, A. I. M. (2004). Simple expressions for normal incidence reflection coefficients from an interface between fluid-saturated porous materials. *Geophysics*, 69:1372–1377.

Gurevich, B., Kelder, O., and Smeulders, D. M. J. (1999). Validation of the slow compressional wave in porous media: Comparison of experiments and numerical simulations. *Transport in Porous Media*, 36:149–160.

Plona, T. (1980). Observation of a second bulk compressional wave in a porous medium at ultrasonic frequencies. *Appl. Phys. Lett.*, 36:259–261.

Rasolofosaon, P. N. J. (1980). Importance of the interface hydraulic condition on the generation of second bulk compressional wave in porous media. *Appl. Phys. Lett.*, 37:898–900.

Rytov, S. M. (1956). Acoustical properties of a thinly laminated medium. *Sov. Phys. Acoust.*, 2:68–80.

Saenger, E. H., Shapiro, S. A., and Keehm, Y. (2005). Seismic effects of viscous Biot-coupling: Finite difference simulations on micro-scale. *Geophys. Res. Lett.*, 32:L14310.